Environment International 137 (2020) 105514

Contents lists available at ScienceDirect

Environment International

journal homepage: www.elsevier.com/locate/envint

Vehicle emissions in a middle-sized city of China: Current status and future trends

Shida Sun[a], Jiaxin Jin[a], Men Xia[b], Yiming Liu[b], Meng Gao[c], Chao Zou[a], Ting Wang[a], Yingchao Lin[a], Lin Wu[a], Hongjun Mao[a,*], Peng Wang[b,*]

[a] Center of Urban Transport Emission Research, College of Environmental Science and Engineering, Nankai University, Tianjin 300071, China
[b] Department of Civil and Environmental Engineering, The Hong Kong Polytechnic University, Hong Kong 999077, China
[c] Department of Geography, Hong Kong Baptist University, Hong Kong 999077, China

ARTICLE INFO

Handling Editor: Xavier Querol

Keywords:
Vehicle emissions
Emission inventory
Emission factors
Policy evaluation
Spatial distribution

ABSTRACT

Vehicle emissions are regarded as an important contributor to urban air pollution in China and most previous studies focused on megacities. However, the vehicle pollution in middle-sized cities becomes more severe due to the increasing vehicle population (VP) and lagged control policy. This study takes Langfang, a typical middle-sized city bordered by two megacities (Beijing and Tianjin), as the target domain to investigate vehicle emissions. The speed correction curves (SCC) are introduced to improve the vehicle emission factors (EF) simulation in official technical guidelines on emission inventory (GEI). A multi-year vehicle emission inventory (from 2011 to 2025) is developed in Langfang. From 2011 to 2017, the total vehicle emissions in Langfang decrease for carbon monoxide (CO), but increase for volatile organic compounds (VOCs), nitrogen oxides (NO_x), and inhalable particles (PM_{10}), respectively. From 2018 to 2025, the emissions would increase more rapidly in Langfang than in Beijing and Tianjin, indicating the middle-sized cities may become a significant contributor to air pollution in China. Four possible control policies, including VP constrained (VPC), public transportation promotion (PTP), new energy vehicles promotion (NEP), and freight transportation structure optimization (FTO) are evaluated. The most significant emissions reductions are observed under the FTO for CO, NO_x, and PM_{10}, and under the VPC for VOCs. The spatial distributions of vehicle emissions show a high order of heterogeneity, indicating that local conditions should be considered in policy formulation in addition to national consistency. More comprehensive policies should be implemented to mitigate the vehicle pollution in middle-sized cities.

1. Introduction

Vehicle emissions are considered as an important contributor to air pollution at global, national, and city levels, causing an adverse effect on air quality and human health (Anenberg et al., 2017). With the rapid urbanization and motorization since the 1990s, vehicles have become a critical source of air pollution in China (Wu et al., 2016; Zheng et al., 2015). The vehicle emissions of nitrogen oxides (NO_x) and volatile organic compounds (VOCs) are recognized as the important precursors of ozone (O_3) and secondary organic aerosol (SOA) in megacities in China (He et al., 2016; Huang et al., 2015; Liu et al., 2017a; Zhao et al., 2012). In recent years, the Ministry of Ecology and Environment of the People's Republic of China (MEE) has established a series of policies to control vehicle pollution, such as scrapping high-emission vehicles and updating vehicular emission standards. These policies have long-term impacts on the amounts and characteristics of vehicle emissions in China (Wu et al., 2016). Therefore, it is necessary to study long-term changes in vehicle emissions.

The multi-year vehicle emission inventory is applied to describe the long-term trends of vehicle emissions and worked as an effective approach to establish control policies (Zhang et al., 2013). In China, a series of multi-year emission inventories were developed at national (Lang et al., 2016; Wang et al., 2011), regional (Song et al., 2016; Sun et al., 2016), and city levels (Wang et al., 2010). Cai and Xie (2013) developed the nationwide multi-year vehicle emission inventories from 2006 to 2009 and suggested that more stringent control policies should be applied in a vast area in China. Liu et al. (2017a) estimated the vehicle emissions in Guangdong from 1994 to 2014 and found a close relationship between the emissions and the gross domestic product (GDP). The multi-year emission inventories at city level were mainly developed in megacities, such as Beijing (Zhang et al., 2014b), Tianjin (Sun et al., 2019), and Guangzhou (Zhang et al., 2013).

* Corresponding authors.
E-mail addresses: hongjunm@nankai.edu.cn (H. Mao), peng.ce.wang@polyu.edu.hk (P. Wang).

https://doi.org/10.1016/j.envint.2020.105514
Received 13 September 2019; Received in revised form 18 January 2020; Accepted 20 January 2020
Available online 05 February 2020

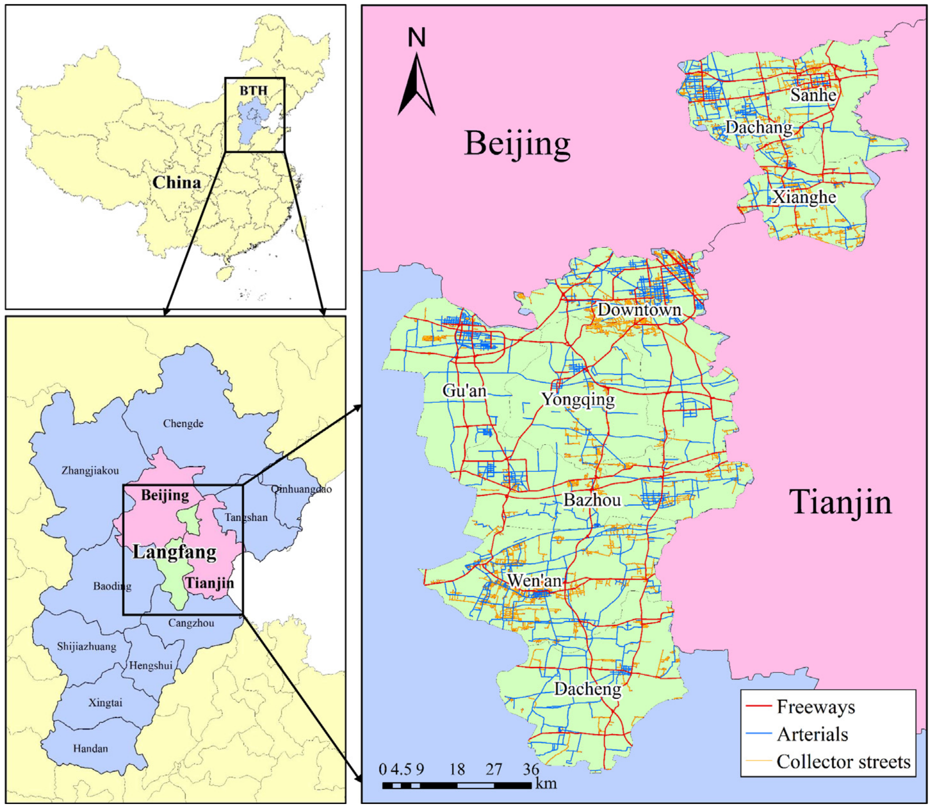

Fig. 1. The location of Langfang in China and the road distributions in Langfang.

As a political, cultural and economic center of China, the Beijing-Tianjin-Hebei (BTH) region has attracted much attention due to the serious air pollution (Xu et al., 2019). Several multi-year vehicle emission inventories have been established in this region (Du et al., 2017; Lang et al., 2012). However, most of them only studied the total emissions in the whole BTH region or focused on the two megacities, Beijing and Tianjin (Peng et al., 2015; Sun et al., 2019; Zhang et al., 2014b). The vehicle emissions in Beijing and Tianjin have been effectively controlled after constraining the vehicle population (VP). By contrast, vehicle pollution in middle-sized and small cities will become more severe due to unconstrained VP (Wu et al., 2017). Langfang is a typical middle-sized city with serious air pollution and located approximately in the midway between Beijing and Tianjin (see Fig. 1). Air pollutants from Langfang have a significant impact on these two megacities by regional transport (Zhao et al., 2018). Previous studies showed that about 28–70% of fine particles ($PM_{2.5}$) and 35–60% of O_3 were attributed to sources outside Beijing (Chang et al., 2018; Streets et al., 2007). Vehicle emissions are an important air pollution source in Langfang considering the large VP with a high increasing rate (Li et al., 2016; Song et al., 2019). The unconstrained VP makes the vehicle emission trends differ from those in the two megacities. The control policies should be formulated in line with local conditions, but the related studies are still lacking. Therefore, it is urgent to study the multi-year vehicle emissions in Langfang, which could help the policymaker to understand the vehicle emissions and adopt more reasonable policies in the BTH region and other middle-sized cities like Langfang.

Also, the accuracy of the vehicle emission inventory plays a significant role in understanding vehicle emission characteristics, which highly depends on the detail level and applicability for basic data, including VP, annual average vehicle kilometers travelled (VKT), and vehicle emission factors (EF) (Wang et al., 2010). In this study, the VP is obtained from the vehicle registration database (VRD) collected by Langfang department of motor vehicles, which provides more detailed VP information than the public data (Song et al., 2016). The VKT is determined based on survey data, which directly reflects the real vehicle activity. The EF is simulated by technical guidelines on emission inventory (GEI) released by MEE (MEE, 2014). Previous studies applied various vehicle emission models in China to simulate EF, such as the computer programme to calculate emissions from road transport (COPERT) (Cai and Xie, 2007), the motor vehicle emission simulator (MOVES) (Pu et al., 2015), and the international vehicle emissions (IVE) (Wang et al., 2008). By comparison with them, GEI is used in this study because it incorporates more local studies (Huang et al., 2017) in China. However, EF simulated by GEI still has some problems. For example, the speed correction factors (SCF) are applied to describe the impact of driving conditions on EF. But based on SCF, the simulated EFs change with speeds discontinuously, which is out of line with reality and should be improved (Jing et al., 2016).

The objectives of this study are to (1) develop the multi-year emission inventory in Langfang from 2011 to 2025; (2) improve the original SCF method using the speed correction curves (SCC); (3) compare the vehicle emissions in Langfang to those in Beijing and Tianjin; (4) evaluate the control policy based on scenario analysis; (5) explore the spatial distributions of vehicle emissions by high-resolution ($0.01^{\circ} \times 0.01^{\circ}$); (6) and quantify the uncertainties in the multi-year emission inventory. The study attempts to provide more comprehensive vehicle control policies, especially for the middle-sized cities, to improve the air quality in China. The research framework is shown in Fig. 2.

2. Method

2.1. Developing vehicle emission inventory

The multi-year (from 2011 to 2025) vehicle emission inventory is developed based on three key parameters: VP, VKT, and EF, using the following equation:

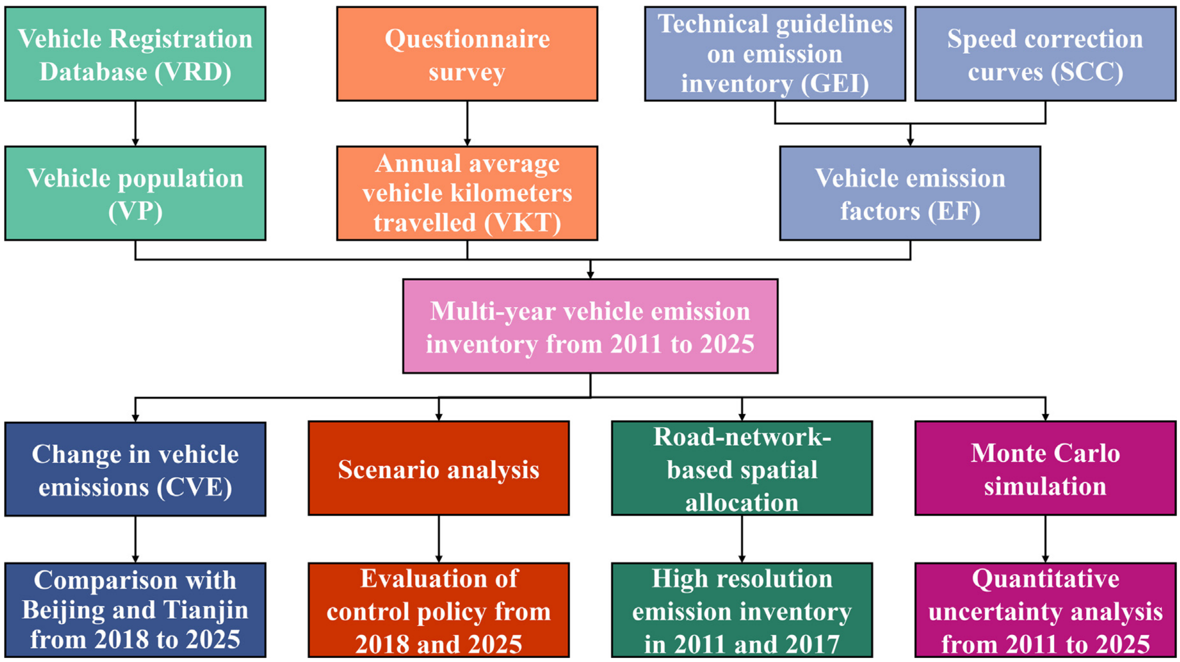

Fig. 2. The research framework for this study.

$$E_p = \sum_{i,j,h} VP_{i,j,h} \times VKT_i \times EF_{i,j,h,p} \times 10^{-9} \quad (1)$$

where E is vehicle emissions; p means a specific pollutant, including four pollutants: carbon monoxide (CO), NO_x, VOCs, and inhalable particles (PM_{10}); i is vehicle types, containing five types: Light-duty passenger vehicle (LDV), Heavy-duty passenger vehicle (HDV), Light-duty truck (LDT), Heavy-duty Truck (HDT), and Motorcycles (MC); j represents fuel types, considering three types: gasoline, diesel, and other fuels; and h means vehicular emission standards, corresponding to pre-China I, China I, China II, China III, China IV, and China V standards. The units of E, VKT, and EF are Gg (10^9 g), km, and g/km, respectively.

The historical VP (from 2011 to 2017) in Langfang is obtained by VRD that recorded detailed properties of local vehicles, including vehicle type (i), fuel type (j), and emission standard (h). The VPs in previous studies (Lv et al., 2019; Sun et al., 2016) were usually collected from public data, such as the government website or statistics yearbook. Most of them only record VP by vehicle type, lacking the detailed VP information, including fuel types and emission standards. Even for the same vehicle type, the EFs are affected by fuel types and emission standards (Vouitsis et al., 2009). Therefore, the detailed VP information is necessary to build corresponding relationships between VP and EF (MEE, 2014). In Beijing and Tianjin, due to lack of VRD data, the detailed VP information is obtained by simulations, using the flowing equation (Lang et al., 2012; Li et al., 2020; Mohammadiha et al., 2018):

$$VP_{i,j,h} = \begin{cases} \sum_y N_{i,j,h,y} & h \neq pre-ChinaI \\ VP_{i,j} - \sum_{h=ChinaI}^{ChinaV} \sum_y N_{i,j,h,y} & h = pre-ChinaI \end{cases} \quad (2)$$

where y is the implementation years of emission standard h for vehicle type i powered by fuel type j (see Fig. S1 for detailed information on implementation years). N is the population of newly registered vehicles. The VP and the new vehicle registrations are obtained from NBSC (2012–2018b) and CATARC (2012–2018).

The VKT is determined according to the survey data. A 500-samples questionnaire survey is conducted to collect VKT in Langfang in 2017, including four major vehicle types: LDV, HDV, LDT, and HDT (total accounts for 99.08% in the whole vehicle fleet). The survey is conducted in communities and parking lots for LDV, in bus stations for HDV, and in toll stations for LDT and HDT. These survey VKTs directly reflect real vehicle activities. GEI also provides default VKT values for each vehicle type. However, these default VKTs are national average values in 2014, which may lead to uncertainties in estimations because VKT varies with both time and locations (Huo et al., 2012). For MC, the in-situ survey is difficult to conduct due to its sparse distribution in Langfang, therefore, its VKT is directly retrieved from GEI. Taking the survey VKT (reflects 2017) as a baseline, the VKTs in other years (from 2011 to 2016, and from 2018 to 2025) are simulated based on their relationship with economy and social development. For LDV, the VKTs are estimated considering its negative relationship with the ownership rate (unit: LDV ownership per person) (Huo et al., 2012). For HDV, LDT, and HDT, the VKTs are derived based on the passenger-kilometers (PKM) and the freight ton-kilometers (FTK) (He et al., 2005). For MC, the VKTs are extrapolated according to the urbanization rate (Cai and Xie, 2013). The related data is obtained from LMBS (2012–2018) and HPBS (2012–2018).

The EF is simulated based on the approach recommended by GEI (MEE, 2014). As the official guidelines in China, GEI incorporates local studies into its approach (Huang et al. 2017). GEI provides a series of base EFs and correction parameters. The base EFs are measured under a standard environment: (1) typical urban driving conditions with average speed of 30 km/h, (2) normal natural environment with temperature of 15 °C, and relative humidity of 50% at low altitudes, (3) sulfur contents of 50 and 350 ppm for gasoline and diesel respectively, (4) and diesel vehicles with load ratio of 50% (MEE, 2014). The correction parameters reflect the impact of relevant factors, such as meteorological conditions and driving conditions, on EF, and are applied to correct base EFs, as the following equation (Liu et al., 2017a):

$$EF_{i,j,h,p} = BEF_{i,j,h,p} \times \varphi_{i,j,h,p} \times \gamma_{i,j,h,p} \times \theta_{i,j,h,p} \quad (3)$$

where BEF is the GEI base EF (g/km); φ, γ, and θ are correction parameters. φ reflects the impacts of meteorological and geographical conditions, including temperature, humidity, and altitude, and all these data (see Table S1) are from LMBS (2012–2018). γ reflects the impact of driving conditions, and the average driving speeds are from previous studies (Song et al., 2018; Sun et al., 2019; Zhang et al., 2013) and shown in Table S2. θ reflects other factors, such as fuel quality and vehicle load. The fuel quality information (see Table S3) is from MEE

(2011–2018). The vehicle load ratio is determined based on the default value. The meanings of other parameters see Eq. (1).

Based on the detailed EFs (differ in vehicle type, fuel type, and emission standard) in Eq. (3), the comprehensive EF (CEF, in g/km) is introduced to reflect the average emission level of a specific pollutant (p) for a vehicle type (i), defined as the following equation (Sun et al., 2017):

$$CEF_{i,p} = \frac{\sum_{j,h} (EF_{i,j,h,p} \times VP_{i,j,h})}{\sum_{j,h} VP_{i,j,h}} \tag{4}$$

meanings of parameters see Eq. (1). CEF is influenced by the composition of fuel types (j) and vehicular emission standards (h).

This study also introduces an improved SCC method in speed correction, which is described in detail in Section 2.2.

2.2. Improving speed correction method

According to GEI, driving conditions are characterized by average speed that is classified into five ranges: < 20 km/h, 20–30 km/h, 30–40 km/h, 40–80 km/h, and > 80 km/h. In the original SCF method, each speed range has a constant γ value (denoted as γ_{scf}). That may cause the following problems: (1) γ_{scf} does not reflect the speed changes when in the same speed range; and (2) γ_{scf} changes discontinuously at the boundary between adjacent speed ranges. Taking VOCs as an example, γ_{scf} for gasoline vehicles are 1.25 and 0.78 in speed ranges of 20–30 km/h and 30–40 km/h, respectively. Accordingly, γ_{scf} is unchanged when speed varies from 20 to 30 km/h, but drops suddenly when the speed is slightly higher than 30 km/h. The simulated EFs are discontinuous based on SCF method, which could not reflect the impacts of driving conditions accurately (Yang et al., 2018).

To solve these problems, an improved SCC method is promoted to obtain consecutive γ values (denoted as γ_{scc}). The SCC uses the quadratic equations (Jing et al., 2016; Liu et al., 2018) as a function of speed V (km/h) as shown in the Eq. (5):

$$\gamma_{scc}(V) = aV^2 + bV + c \tag{5}$$

where a, b, and c are empirical parameters determined by fitting the original γ_{scf} values which are assumed to represent the median values from the matched speed ranges. For instance, when the $\gamma_{scf} = 1.25$ (from 20 to 30 km/h), the corresponding speed is 25 km/h in the SCC method. For speed range of > 80 km/h, the speed V is assumed as 90 km/h. The relationship between γ_{scf} and average speeds is re-defined by the Eq. (5) using SCC, and therefore EF could change with speed continually.

2.3. Predicting future vehicle emissions

The predictions consist of two parts. The future vehicle emissions (from 2018 to 2025) are predicted (1) under the business-as-usual scenario (BAU) in Langfang, Beijing, and Tianjin to draw a comparison between the middle-sized cities and the megacities, (2) and under the BAU and five control scenarios in Langfang to evaluate the emission control policies. The future emissions are also estimated using Eq. (1). Therefore, the predictions on VP, VKT, and EF are required.

The BAU is a reference scenario. The vehicles are naturally eliminated, and the control policies remain unchanged as the base year (2017). For example, according to the current policy, the VP is constrained in Beijing and Tianjin but unconstrained in Langfang, which is considered and remains in force during the whole predicted period. The VP is predicted based on its relationship to GDP, using the elastic coefficient method (Liu et al., 2017b). The VKT is extrapolated by the methods described in Section 2.1. The EF is simulated based on Eq. (3), by assuming the newly registered vehicles meet the latest emission standards in 2017. Other input data for the predictions, such as GDP, population, PKM, FTK, and urbanization rate, are assumed to follow their historical trends (HPBS, 2012–2018; LMBS, 2012–2018; NBSC, 2012–2018b) without new policy interventions.

So far (in 2017) the VP in Langfang is significantly lower than that in Beijing and Tianjin. Therefore, the predicted emissions would be certainly lower in Langfang than in Beijing and Tianjin. Considering this, the change in vehicle emissions (CVE) is introduced for the comparison, given by the following equation:

$$CVE_{p,y} = E_{p,t} - E_{p,t-1} \tag{6}$$

where CVE (Gg) reflects the difference in vehicle emissions (E) between the estimated year (t, from 2018 to 2025) and the previous year (t-1).

The control scenario is designed by incorporating additional emission control policies into the BAU and used to evaluate the effects of policies. Several traditional policies, such as updating emission standards, scrapping high-emissions vehicles, and improving fuel quality, have been introduced and achieved some positive effects over the past decade (Du et al., 2017; Liu et al., 2017b; Zhang et al., 2014a). This study focuses on four possible control policies that are newly (or will be) implemented. First, VP constrained (VPC). The VP is currently constrained by the license registration control in Beijing and Tianjin, which is regarded as an effective way to simultaneously reduce emissions and ease congestion (Zhang et al., 2014b). Second, public transportation promotion (PTP). Public transportation, including the city bus, subway, and light rail, is developed rapidly in recent years. As a clean and efficient travel mode, the penetration of public transportation would further increase, especially in the middle-sized cities where the mass transit is not highly developed (PGHP, 2017). Third, new energy vehicles promotion (NEP). The new energy vehicles in this study refer to the battery electric vehicles and fuel cell vehicles (BMSTC, 2018). Some incentive policies are issued to encourage the production, sale, purchase, and use of new energy vehicles, including subsidies and tax exemptions (Wu et al., 2017). Fourth, freight transportation structure optimization (FTO). The highway remains the dominant mode in freight transportation, leading to serious air pollution and low energy efficiency (Song et al., 2018). The optimization of freight transportation is introduced as a promising way to mitigate vehicle emissions, improve transport efficiency and reduce logistics cost (GOSC, 2018). The optimization is performed by partly shifting freight traffic from highways to railways and waterways.

Besides, the integrated scenario (IS) is introduced by combining all control policies mentioned above to evaluate the comprehensive

Table 1
Detailed definitions of different scenarios from 2018 to 2025 in Langfang.

Scenario	Detailed definition
BAU	Keep the vehicles naturally eliminated and the control policies unchanged as 2017.
VPC	The annual increasing rate of LDV is set at 5%.
PTP	The VKTs of LDV are lower than those under the BAU. The differences are 0 and 25% in 2017 and 2025, respectively. For other years, the values are obtained by interpolation.
NEP	The proportions of new energy vehicles in LDV and HDV registrations are 20% and 30% from 2018 to 2020 and increase to 30% and 50% from 2021 to 2025.
FTO	The VPs and the VKTs are lower than those under the BAU for LDT and HDT. The differences are 0 and 12% in 2017 and 2025, respectively. For other years, the values are obtained by interpolation.
IS	The control policies in VPC, PTP, NEP, and FTO are integrated.

effects, which is expected to achieve the maximum emission reductions. Therefore, a total of six scenarios are considered, including BAU, VPC, PTP, NEP, FTO, and IS. The detailed definitions are summarized in Table 1.

The effects of control scenario are evaluated by the reduction rates of vehicle emissions compared to BAU (RRB), given by the following equation (Sun et al., 2019):

$$RRB_{\mathrm{cs,p,t}} = \frac{E_{BAU,p,t} - E_{cs,p,t}}{E_{BAU,p,t}} \tag{7}$$

where *cs* is the control scenario (including VPC, PTP, NEP, FTO, and IS), *E* means vehicle emissions of pollutant *p* under the BAU or control scenarios (*cs*) in the predicted year *t*. The average RRB (ARRB) reflects the general control effects, calculated by dividing the total RRB by time length (8 years between 2018 and 2025) during the whole predicted period.

2.4. Exploring spatial distributions

The high resolution gridded emission inventory is developed based on "the road-network-based approach", proposed by Zheng et al. (2012). This method introduces a comprehensive spatial surrogate considering traffic flows, road lengths, and emission intensities. The annual total emissions are re-projected and then re-gridded to target domain with a horizontal resolution of 0.01° × 0.01°, which is processed in the following steps:

(1) Establish the target domain. By using Geographical Information Systems (ArcGIS 10.4.1), digital road-network map of Langfang (latitudes: 38°28′26.2″ N − 40°5′8.1″ N, and longitudes: 116°6′20.3″ E − 117°15′9.9″ E) is re-gridded into 7112 grids with 0.01°×0.01° resolution, as shown in Fig. S2.
(2) Calculate actual road length. Lengths of different road types (freeways, arterials, and collector streets) at city, county, and grid levels are calculated through ArcGIS.
(3) Estimate road conversion coefficients (RCC). The RCC is determined by the ratio of traffic flow between the actual road and the standard road, as the following equation:

$$RCC_r = \frac{TF_r}{STF} \tag{8}$$

where *r* represents the specific road type; *TF* and *STF* are the traffic flow (on the actual road) and standard traffic flow (on the standard road), respectively. The *STF* is a user-defined constant (Zheng et al., 2012).

(4) Convert actual road lengths to standard road lengths. The total standard road lengths are determined based on the actual road lengths and the RCC, as the following equation:

$$TSRL_a = \sum_r (ARL_{a,r} \times RCC_r) \tag{9}$$

where *a* represents the target areas which are at county level in this study, including downtown and eight counties. *TSRL* and *ARL* are total standard road lengths (km) and actual road lengths (km), respectively.

(5) Determine the standard emission intensity. Total emissions at city level are re-distributed to county level by VP distribution. And the standard emission intensities are determined by total emissions and standard road lengths at county level, as the following equation:

$$SEI_a = \frac{E_a}{TSRL_a} \tag{10}$$

where *SEI* is standard emission intensity (t/km); *E* represents vehicle emissions (t).

(6) Simulate gridded emissions. Based on RCC, the actual road lengths in each grid are converted to standard road lengths, then the vehicle emissions are simulated at grid level, as the following equation:

$$E_{a,g} = SEI_a \times \sum_r (ARL_{a,g,r} \times RCC_r) \tag{11}$$

where *g* represents the grid cell number.

2.5. Quantifying multi-year uncertainties

Uncertainties are inevitable in multi-year emission inventory, for two reasons: (1) the estimation method simplifies actual emission process; (2) the input data (VP, VKT, and EF) has uncertainties and difficult to determine (Gong et al., 2017). For example, the EF changes simultaneously with the vehicle speed (Suarez-Bertoa et al., 2016). The real speeds are changing continuously but simplified as the average speed in simulations, which leads to uncertainties in EF. Quantifying uncertainties would identify the key factors to improve data collections and emission estimations (IPCC, 2006).

Monte Carlo simulation is introduced to quantify the uncertainties, which is recommended by IPCC (2006) and has been widely used in China (Cai and Xie, 2013). The emissions uncertainties are quantified based on the relationship between emissions and input data (VP, VKT, and EF) as shown in Eq. (1). The input data uncertainties are described by the probability distribution and the coefficients of variation (CV, the standard deviation divided by the mean).

The normal distribution with CV of 5% is set for the historical VP (from VRD) and 10% for the future VP (predicted values), considering the different uncertainties within the data sources (Sun et al., 2019). The uncertainties of VKT are determined based on the in-situ survey for LDV, HDV, LDT, and HDT. For MC the related parameters are specified according to Lang et al. (2016). As for EF, the probability distribution and CV are gathered from previous studies (Guo et al., 2016; Lang et al., 2014). The details are illustrated in Table 2. The prognosis of Monto Carlo simulation is also significantly influenced by the trial number, which is set to 10,000 to ensure accuracy (Hao and Song, 2018). The emission uncertainties are quantified year by year and then aggregated to determine the multi-year uncertainties.

3. Results and discussion

3.1. Summary of vehicle activity

Fig. 3 shows the vehicle activity data used in Eq. (1), including VP (panel (a) and (b)) and VKT (panel (c) and (d)). The future VP (from 2018 to 2025) is determined under the BAU. More detailed information on VP, including vehicle types, fuel types, and vehicular emission standards, is illustrated in Fig. S3.

The VP increases from 830.5 to 1225.2 thousand between 2011 and 2017 in Langfang. LDV dominates the vehicle fleet (as high as 86.0% in 2017). From 2014 to 2017, the LDV increases much higher in Langfang

Table 2
The setting for the probability distribution and the CV in Monte Carlo simulation.

Independent variable			Probability distribution	CV
VP	2011–2017		Normal distribution	5%
	2018–2025		Normal distribution	10%
VKT	LDV		Normal distribution	41.2%
	HDV		Normal distribution	11.8%
	LDT		Normal distribution	41.4%
	HDT		Normal distribution	52.7%
	MC		Normal distribution	30%
EF	CO, NO_x, VOCs	Pre-China I, China I	Lognormal distribution	36%
		China II-China V	Lognormal distribution	17%
	PM_{10}	Pre-China I, China I	Lognormal distribution	59%
		China II-China V	Lognormal distribution	34%

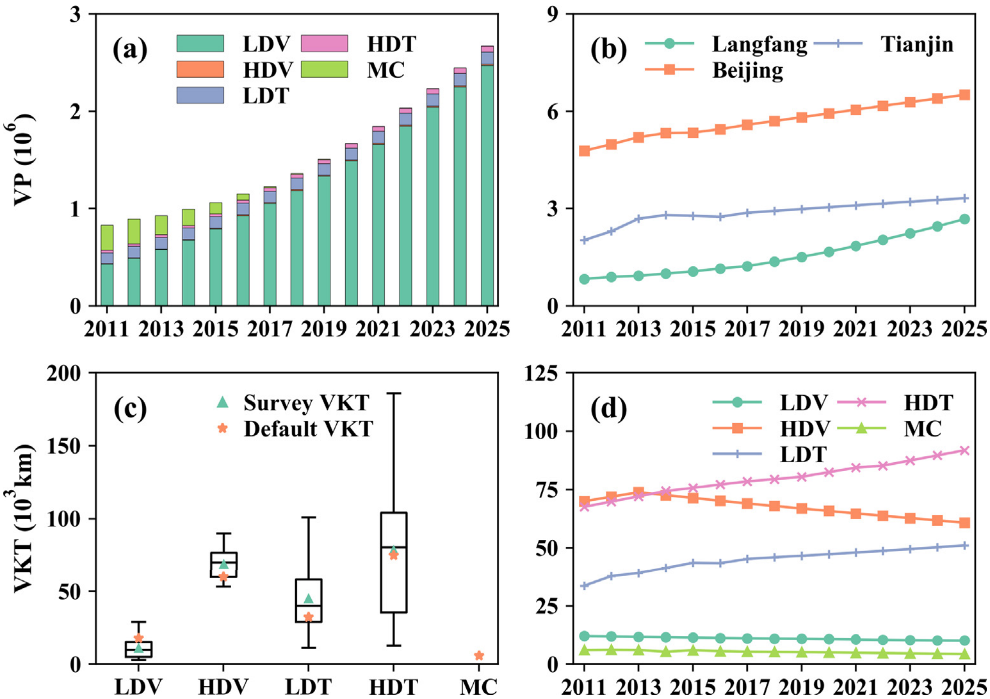

Fig. 3. Vehicle activity data: (a) the VP by vehicle type in Langfang, (b) the VP in Langfang, Beijing, and Tianjin, (c) the survey VKTs in Langfang and the GEI default VKTs, and (d) the trends of VKT in Langfang.

(increases by 55.7%) than that in Beijing (5.3%) and Tianjin (3.7%) (see Fig. S3). The implementation of the VP constrained policy (2011 and 2014 for Beijing and Tianjin respectively) accounts for the lower increasing rates (NBSC, 2012–2018b). For HDV, the population significantly increases by 46.8% from 2011 to 2017 in Langfang due to promoting public transportation (Peng et al., 2015). For LDT, the increasing rate is significantly lower in Langfang (5.2%) than that in Beijing (93.9%) and Tianjin (60.1%) (see Fig. S3). However, a slightly higher increasing rate of HDT is observed in Langfang (30.3%; 29.6% and 23.9% for Beijing and Tianjin respectively). The HDT increases more rapidly in the middle-sized city because of the constrained policy in megacities (Wu et al., 2017). MC is an important contributor to the total VP in 2011 (accounts for 30.8%) but becomes negligible in 2017 (0.9%), due to the stringent restrictions on MC in urban areas (Wang et al., 2010).

In future simulations, the total VPs are predicted to increase by 96.5%, 14.2%, and 13.4% in Langfang, Beijing, and Tianjin, respectively. LDV is a driving force for the total VP and increases much faster in Langfang (108.3%) than that in Beijing (10.4%) and Tianjin (11.1%). In China, the LDV will continue to increase rapidly in the next decade, especially in middle-sized and small cities, such as Langfang, leading to an increase in energy consumption, congestion, and pollution (Du et al., 2017). The increasing rate of the HDV in Langfang (39.9%) is higher than in Beijing (11.9%) and Tianjin (0.5%) indicating the higher development rate of public transportation in Langfang in the future. With more prosperous freight transportation in the megacities, higher increasing rates of LDT are observed in Beijing (79.5%) and Tianjin (34.7%) compared to that in Langfang (7.8%). However, Langfang has the highest increasing rate of HDT (54.5%) compared to Beijing (24.7%) and Tianjin (32.2%) due to the constraints on HDT registration in megacities. Considering the restrictions in urban areas, MC would decrease by 83.9% in Langfang, 47.9% in Beijing, and 78.0% in Tianjin.

The survey conducted in Langfang in 2017 shows the VKTs are 78493, 69009, 45239, and 11111 km for HDT, HDV, LDT, and LDV, respectively. Compared to default VKT (from GEI), the survey VKTs are 38.3% lower for LDV while 15.0%, 39.2%, and 4.7% higher for HDV, LDT, and HDT, respectively. For LDV, the VKT negatively correlates with the ownership rate (Huo et al., 2012). The LDV ownership rate in Langfang (0.22) is higher than the national average (0.13) (NBSC, 2012-2018b), leading to lower VKT value. Beijing Transport Institute (BTI) conducted a 2000-samples VKT survey in Beijing in 2018 and indicated the VKT of LDV is 11968 km, which is comparable with the results (11111 km) in this study. For other vehicle types, the differences between the survey VKTs and the GEI default values are mainly attributed to transportation development and local conditions. The VKT of MC is not obtained by surveys due to its sparse distribution, and consequently, the GEI default VKT (6000 km) is used in the emission estimations.

Taking survey VKTs (year 2017) as the baseline, VKTs in other years are simulated using the methods described in Section 2.1. From 2011 to 2025, the VKTs decrease by 15.1%, 13.2%, and 27.8% for LDV, HDV, and MC, while increase by 51.8% and 35.8% for LDT and HDT, respectively. The popularized private cars lead to the VKT decrease for LDV (Sun et al., 2019). The VKT of HDV decreases from 2013 due to the decline in highway passenger transportation (HPBS, 2012-2018). By contrast, railway passenger transportation develops rapidly. An increasing number of people choose to travel by train in recent years, especially for long-distance journeys (NBSC, 2012-2018b). Given this, the VKT of HDV is expected to decrease in the future. The VKT of MC decreases with the urbanization process since the MC is restricted in urban areas (Cai and Xie, 2013). The VKTs of LDT and HDT increase continually, caused by the rapid development of freight transportation (Guo et al., 2016). Unlike highway passenger transportation, the highway freight volume increases rapidly with economic development, both locally and nationally (LMBS, 2012-2018).

3.2. Difference between SCF and SCC

This section takes VOCs as an example to discuss the difference between using SCF and SCC. Fig. 4(a) shows the γ determined by SCF (γ_{scf}) and SCC (γ_{scc}), respectively, for the gasoline vehicles. The γ_{scf} in five speed ranges are fitted using Eq. (5) to calculate the empirical parameters of SCC equation, expressed as $\gamma_{scc} = 0.0004\ V^2 - 0.0565\ V + 2.27$. More information of SCC is presented in Table S4.

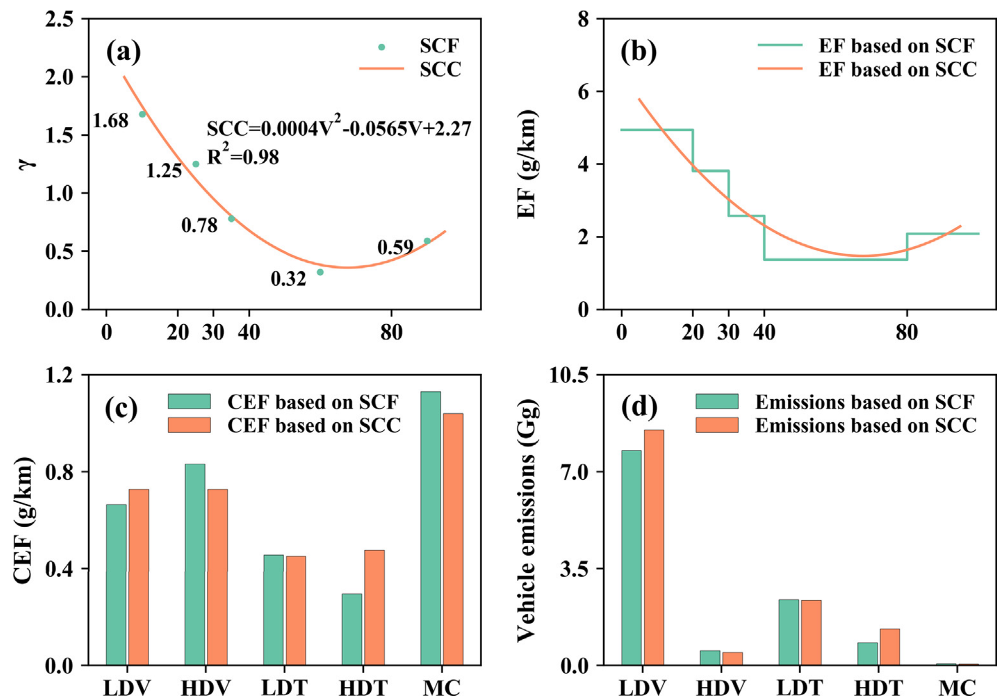

Fig. 4. (a) γ, (b) EF, (c) CEF, and (d) vehicle emissions of VOCs based on SCF and SCC in Langfang in 2017.

Taking gasoline LDV with pre-China I as an example, Fig. 4(b) compares the EFs by using the SCF and SCC methods. The EFs are 2.6 and 2.9 g/km, based on SCF (γ_{scf} = 0.78) and SCC (γ_{scc} = 0.89), respectively with the average speed of 32 km/h.

The detailed EFs are aggregated to obtain CEF using Eq. (4). Fig. 4(c) shows the CEF in 2017 based on SCF and SCC methods. The most significant difference is observed in HDT, and the CEF of SCC (0.48 g/km) is 60.7% higher than that of SCF (0.3 g/km) method. The CEFs of other pollutants are illustrated in Fig. S4. Fig. 4(d) shows the differences in vehicle emissions caused by method selection. The total emissions based on SCF are 9.0% lower than on SCC, indicating that using SCF method may underestimate VOCs emissions. As for vehicle types, the most significant emission difference is observed in LDV, for which the emissions based on SCF are 0.7 Gg lower than those on SCC, indicating an underestimation of VOCs emissions in urban areas that have higher LDV population. For other pollutants, comparisons of emissions are shown in Fig. S5.

The SCF calculated EFs change significantly at the speed ranges boundaries. Introducing SCC converts these discrete EFs into a continuous trend, which is more representative of the real-world situations (Wu et al., 2015; Yang et al., 2018). Therefore, the EFs used for emission estimations are simulated based on SCC in the following sections.

3.3. Trends in vehicle emissions

Fig. 5 shows the vehicle emissions from 2011 to 2025 in Langfang. The future emissions (from 2018 to 2025) are displayed under the BAU scenario. The vehicle emissions during the same period in Beijing and Tianjin are illustrated in Figs. S6 and S7.

The CO emissions decrease from 60.4 to 46.6 Gg in Langfang from 2011 to 2017. CO emissions are mitigated in most of China by updating emission standards (Liu et al., 2017a). However, the decreasing rate (22.9%) in Langfang is lower than in Beijing (66.2%) and Tianjin (63.5%) due to the control policy lags (Jia et al., 2018). First, emission standards in middle-sized cities are usually updated later than in megacities (Wu et al., 2017). For example, the China V standard for LDV was implemented from 2016 in Langfang but from 2013 in Beijing. Second, the VP is unconstrained in middle-sized cities while constrained in megacities. Constraints on VP play an important role in mitigating vehicle emissions in Beijing and Tianjin (Sun et al., 2019; Zhang et al., 2014b). In the future, the CO emissions in Langfang would decrease to 41.6 Gg in 2020 and then rebound to 45.6 Gg in 2025 due to the high VP increasing rate. The LDV (accounts for 38.3%), LDT (36.1%), and HDT (17.6%) are important contributors to CO emissions from 2011 to 2025. The LDV is usually a dominant contributor to CO emissions (Huo et al., 2011; Jing et al., 2016). However, the LDT and HDT are also major contributors to CO emissions, and their contributions would increase in the future due to relatively high EFs and VKTs.

The VOCs emissions are fluctuant between 2011 and 2017. However, the VOCs emissions decrease significantly in Beijing (decrease by 52.7%) and Tianjin (50.3%) during the same period. The difference is mainly attributed to the VP constrained policy. The VOCs emissions are not reduced in Langfang although the stringent emission standards are implemented, because the reductions have been offset due to the unconstrained VP (increase 47.5%). By contrast, the VOCs emissions in Tianjin decrease slowly (8.6% from 2011 to 2013) before constraining VP, and more rapidly (38.3% from 2014 to 2017) after that. In the future, the VOCs emissions in Langfang would increase to 16.7 Gg in 2025. LDV is the most important contributor to VOCs emissions, with an increasing contribution from 51.6% in 2011 to 74.7% in 2025. Most LDVs (98.9%) are gasoline vehicles that have two important sources of VOCs: exhaust emissions and evaporative emissions (Li et al., 2015). The past emission standards mainly focused on exhaust emissions control. However, the evaporative emissions now become the dominant source of vehicle VOCs emissions (Liu et al., 2015), especially for LDV, which should arouse public concerns.

NO_x is the only pollutant with the obvious increasing trend from 22.2 Gg in 2011 to 25.7 Gg in 2017. Reducing NO_x emissions is difficult not only in Langfang, but also in Beijing and Tianjin. Updated emission standards are the major policy to control vehicle pollution, but have limited impacts on NO_x emissions control in the past (Shen et al., 2015). Most (nearly 90%) NO_x emissions are contributed by the diesel vehicles in Langfang. According to the data from portable emission measurement systems (PEMS), no statistical reductions are observed in the real-world NO_x emissions for diesel trucks from China I to China III standards, although the emission limits are tighter (Wu et al., 2016). As a

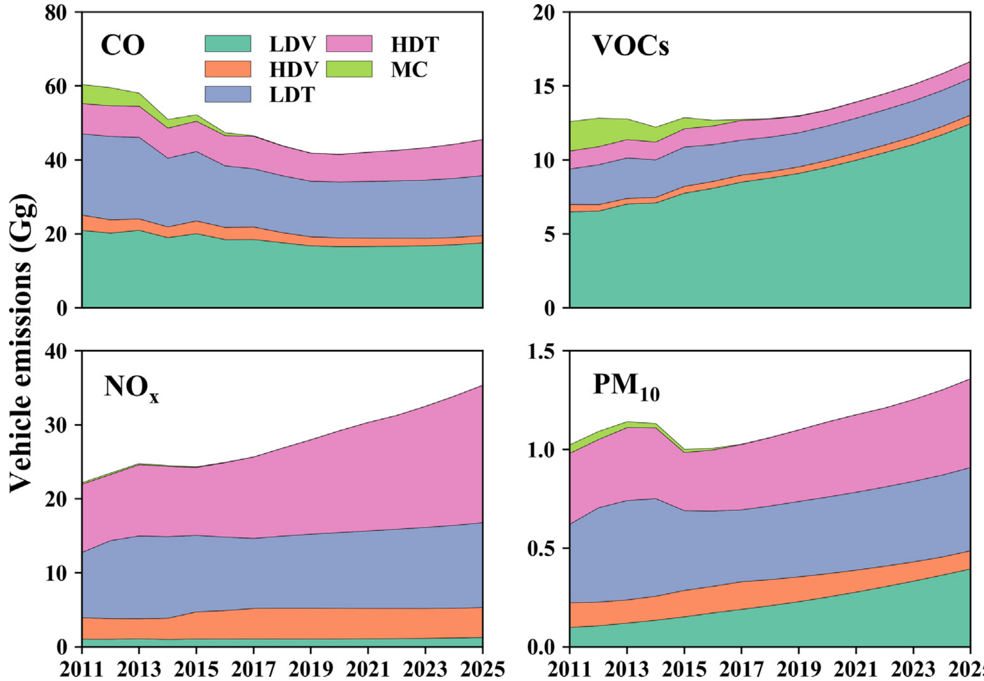

Fig. 5. Vehicle emissions in Langfang from 2011 to 2025.

result, the gap between the on-road EF and emission limits becomes larger and larger (Wu et al., 2012). Even in 2017, 60.1% of diesel vehicles do not meet the China IV (and above) standard. These vehicles should be scrapped as soon as possible for effectively reducing NO_x emissions. Besides, the China VI standard will be implemented in 2020, which is expected to have more significant impacts on NO_x emissions control (Wu et al., 2017). The predictions show the NO_x emissions in Langfang would increase to 35.4 Gg in 2025. LDT (accounts for 37.9%) and HDT (44.5%) are the major contributors to NO_x emissions. Their contributions to NO_x emissions increase along with freight transportation development, in which the road traffic still has an important role to play (Song et al., 2018).

The PM_{10} emissions increase from 1.02 to 1.13 Gg during 2011 to 2014 then decrease to 1.03 Gg in 2017. However, in Beijing and Tianjin, the PM_{10} emissions decrease 40.9% and 60.1%, respectively. Diesel vehicles are also a dominant contributor (accounts for 77.0%) to PM_{10} emissions. The increase of PM_{10} emissions in Langfang is caused by the rapid growth in HDV and HDT, and most (75.2%) of them are powered by diesel. The highest decreasing rate occurs between 2014 and 2015 (as high as 0.13 Gg), which is mainly benefited from improving fuel quality. The sulfur content of diesel decreases from 350 to 50 ppm (Lang et al., 2016), leading to the decrease of θ (see Eq. (3)), and therefore the emissions from diesel vehicles are reduced by 0.15 Gg (Wang et al., 2016). The PM_{10} emissions in Langfang are predicted to increase to 1.36 Gg in 2025. The LDT (accounts for 36.7%) and HDT (32.5%) are also major contributors to PM_{10} emissions, which indicates PM_{10} and NO_x emissions have the same major contributors. The PM_{10} emissions from vehicles are currently becoming an important source of ambient particulate matter and should be effectively controlled (Fang et al., 2017).

3.4. Comparison of future trends

Despite the higher VP increasing rate, total emissions in Langfang are lower than in Beijing and Tianjin during the predicted period (see Fig. S8). However, the CVEs are comparable in the three cities and shown in Fig. 6.

From 2021 to 2025, the CO emissions in Langfang increase with higher CVEs than in Beijing and Tianjin. The VOCs emissions increase (positive CVEs) in Langfang during the whole prediction period, while decrease (negative CVEs) in Beijing and Tianjin most of the time. The results indicate, in the future, the vehicle emissions in middle-sized cities would increase more rapidly than those in megacities. The current VP constrained policy focuses on LDV that is the dominant contributor in the vehicle fleet. From 2018 to 2025, the CO emissions from LDV are nearly constant in Langfang (decrease by 0.3%) but decrease significantly in Beijing (14.0%) and Tianjin (11.9%). At the same time, their VOCs emissions increase significantly in Langfang (41.8%) but decrease in Beijing (4.1%) and Tianjin (5.7%). With VP constrained, the emissions are reduced in the megacities as new vehicles (stringent standard with low emissions) registered and old vehicles (high emissions) scrapped. By contrast, VP is unconstrained in middle-sized cities, leading to rapid emissions increase.

The NO_x and PM_{10} emissions in Langfang keep increasing from 2018 to 2025. Remarkably, the NO_x emissions in Beijing and Tianjin would increase more rapidly (higher CVE) than those in Langfang from 2022 and 2020, respectively. And the close CVEs in PM_{10} emissions are observed in all these cities at the end. The results suggest the NO_x and PM_{10} emissions would become a serious problem both in middle-sized cities and megacities. The LDT and HDT are a driving force to the increasing NO_x and PM_{10} emissions, contributing more than half in Langfang (84.9% and 64.1%), Beijing (66.9% and 53.9%), and Tianjin (81.4% and 67.4%) in 2025. It is impractical to control LDT and HDT population because they still play an important role in freight transportation that is essential for sound economic development (NBSC, 2012-2018b). Considering the policy lags, the situation is even worse in middle-sized cities, where the emission standards are generally lower than in megacities. The share of LDT and HDT with high emission standards (China IV and China V) is 65.7% in Langfang in 2025, lower than Beijing (97.9%) and Tianjin (92.2%).

To summarize, the CO and VOCs emissions would continue to increase in Langfang and be reduced in Beijing and Tianjin, demonstrating VP constrained is an effective way to control vehicle pollution. And the reduction in NO_x and PM_{10} emissions would be more challenging both in middle-sized cities and megacities due to freight transportation development. More innovative and comprehensive policies should be formulated and implemented to control vehicle emissions.

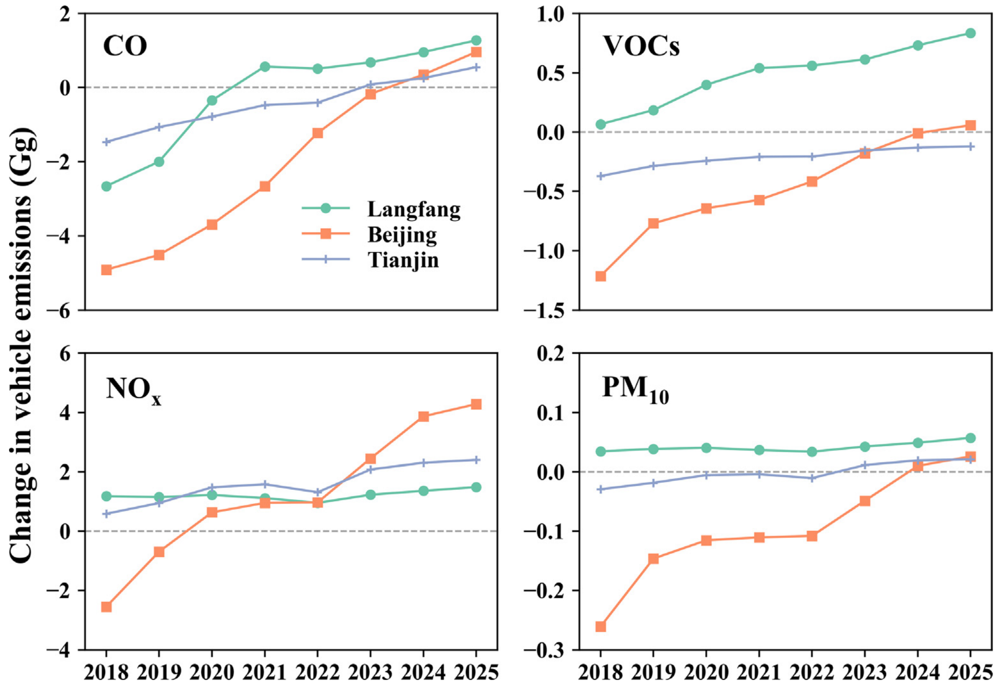

Fig. 6. Change in vehicle emissions (CVEs) in Langfang, Beijing, and Tianjin from 2018 to 2025.

3.5. Evaluation of control policies

Fig. 7 shows the future vehicle emissions (from 2018 to 2025) in Langfang under the BAU and five control scenarios. Unsurprisingly, the most significant reductions are observed in the IS, under which the ARRBs are 16.0%, 25.0%, 14.7%, and 20.5% for CO, VOCs, NO_x, and PM_{10} emissions, respectively. As for a single policy, the control effects vary for different pollutants.

The FTO is the most effective control policy for CO emissions, with the highest ARRB of 8.3%. Because the LDT and HDT would become important contributors (total contribution of 57.0% in 2025) to CO emissions under the BAU. Optimizing freight transportation would help to lower the vehicle activity of LDT and HDT, and reduce their emissions by 23.2% and 18.0%, respectively, from 2017 to 2025. PTP also plays a key role (ARRB of 5.5%). By improving public transport, the usage rate of LDV would be reduced, and consequently, their CO emissions decrease 28.8% in the same period.

The VPC (ARRB of 10.5%) and PTP (10.3%) are more effective control policies for VOCs emissions due to lowering the VP and VKT for LDV. The LDV is a dominant contributor (contribution of 74.7% in 2025) to VOCs emissions. Compared to 46.3% under BAU, the VOCs emissions from LDV would increase only 8.4% (under VPC) by constraining VP, and 9.8% (under PTP) by promoting public transportation, from 2017 to 2025. In short, reducing the use of LDV is essential

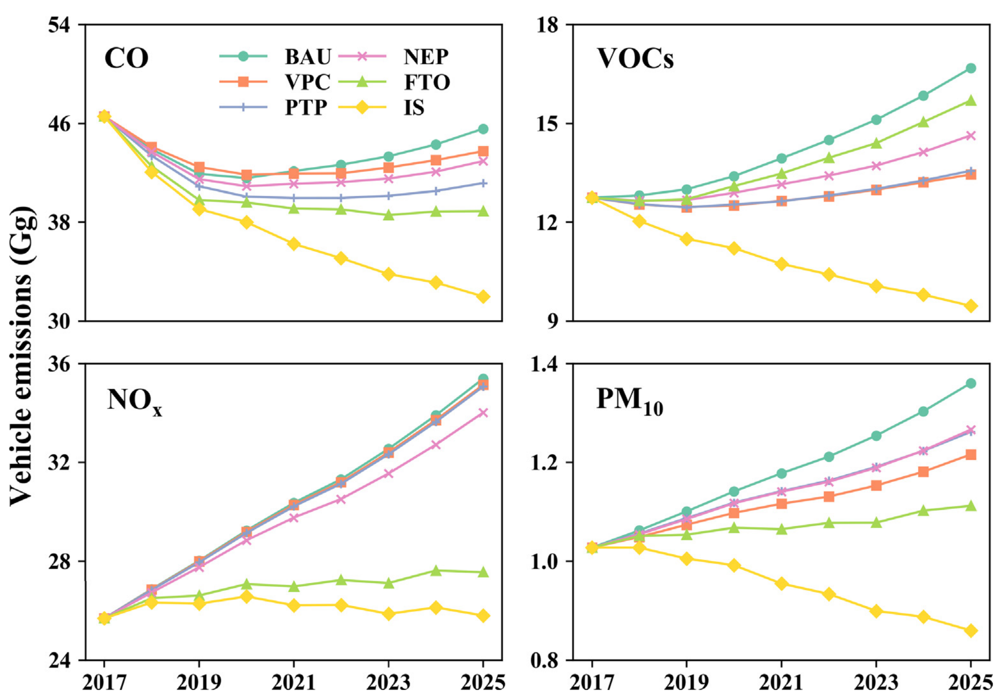

Fig. 7. Vehicle emissions in Langfang from 2017 to 2025 under different scenarios.

for VOCs emissions control. Promoting the new energy vehicles (NEP; ARRB is 6.6%) is also a promising policy. The RRB increases rapidly from 1.2% in 2018 to 12.2% in 2025, indicating the long-term gains under the NEP.

The FTO has a significant effect on controlling NO_x emissions, with a higher ARRB of 11.9%. Most NO_x emissions (84.9% in 2025) come from LDT and HDT. Under the FTO, the VP and VKT are expected to simultaneously decrease for LDT and HDT, inhibiting the increasing NO_x emissions (increase by 8.5% vs. 46.8% under the BAU, from 2017 to 2025). The NEP (ARRB of 2.2%) is also an effective way to control NO_x emissions. By promoting the new energy vehicles, the NO_x emissions from HDV (contributes 11.5% in 2025) would decrease 30.6%.

The FTO also has the greatest effect (ARRB of 10.0%) on reducing PM_{10} emissions. The LDT and HDT (major contributors to NO_x and PM_{10}) emissions are a knotty problem both in middle-sized cities and megacities. The optimization of freight transportation structures would produce co-reduction effects on NO_x and PM_{10} emissions simultaneously. Also, the VPC (ARRB of 5.9%) has a positive effect on PM_{10} emissions control. For LDV, the PM_{10} emissions would increase more slowly under the VPC (increase by 31.7%) than the BAU (107.6%).

3.6. Characteristics of spatial distribution

The total vehicle emissions in Langfang in 2011 and 2017 are first allocated at county level (see Fig. 8), and then re-gridded to 0.01°×0.01° resolution (see Fig. 9). The vehicle emissions show a significant discrepancy at county level. High emission areas are mainly located at Downtown, Sanhe, and Bazhou, with the contribution of > 54% to total emissions. Even for the same pollutant, the dominant contributors are various in different counties. Taking CO as an example, in 2017, the dominant contributors are LDV (in Sanhe, Dachang, Xianghe, Yongqing, Gu'an, Bazhou, and Dacheng) and LDT (in Downtown and Wen'an). The detailed emission contributions by vehicle types are presented in Table S5. The results suggest local conditions should be considered in policy formulation in addition to national consistency. Between 2011 and 2017, the most significant vehicle emissions reductions are observed in Bazhou for CO (3.6 Gg), VOCs (0.3 Gg), and PM_{10} (0.03 Gg), and in Sanhe for NO_x (0.3 Gg). By contrast, the most significant increase occurs in Dacheng for CO (0.2 Gg) and PM_{10} (0.04 Gg), and in Downtown for VOCs (0.3 Gg) and NO_x (2 Gg). The counties with significantly increased emissions should be regarded as the key areas in policy formulation.

The emissions at county level are further allocated at grid level considering the traffic flows, road lengths, and emission intensities. Several spatial surrogates were applied to allocate emissions in previous studies (Cai and Xie, 2007; Sun et al., 2016), such as population and road density. However, the population distribution and road density do not reflect vehicle activities and road loading comprehensively (Alam et al., 2018), which introduces bias in the emission allocations (Gong et al., 2017). In this study, not only the road distribution but also the traffic flows and fleet compositions are considered to conduct the emission distribution. The gridded emissions are consistent with the road network and reflect the difference between the road types. The grids with high emissions are mainly located in city centers along freeways and arterials. Overall, using "the road-network-based approach" provides more accurate information than single spatial surrogate.

3.7. Multi-year uncertainties

Fig. 10 shows the uncertainty analysis and the results from other studies for vehicle emissions in Langfang. So far, few studies have focused on middle-sized cities, including Langfang. This study compares the results with two nationwide emission inventories, the China Vehicle

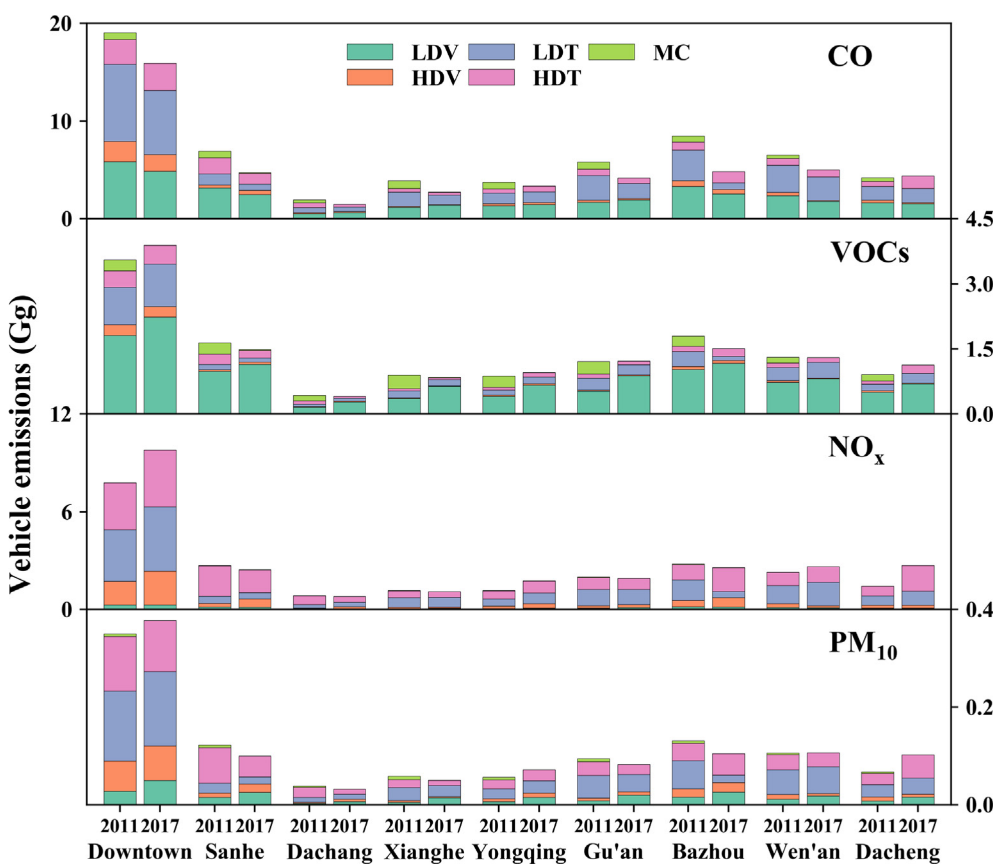

Fig. 8. Vehicle emissions at county level in Langfang for years 2011 and 2017.

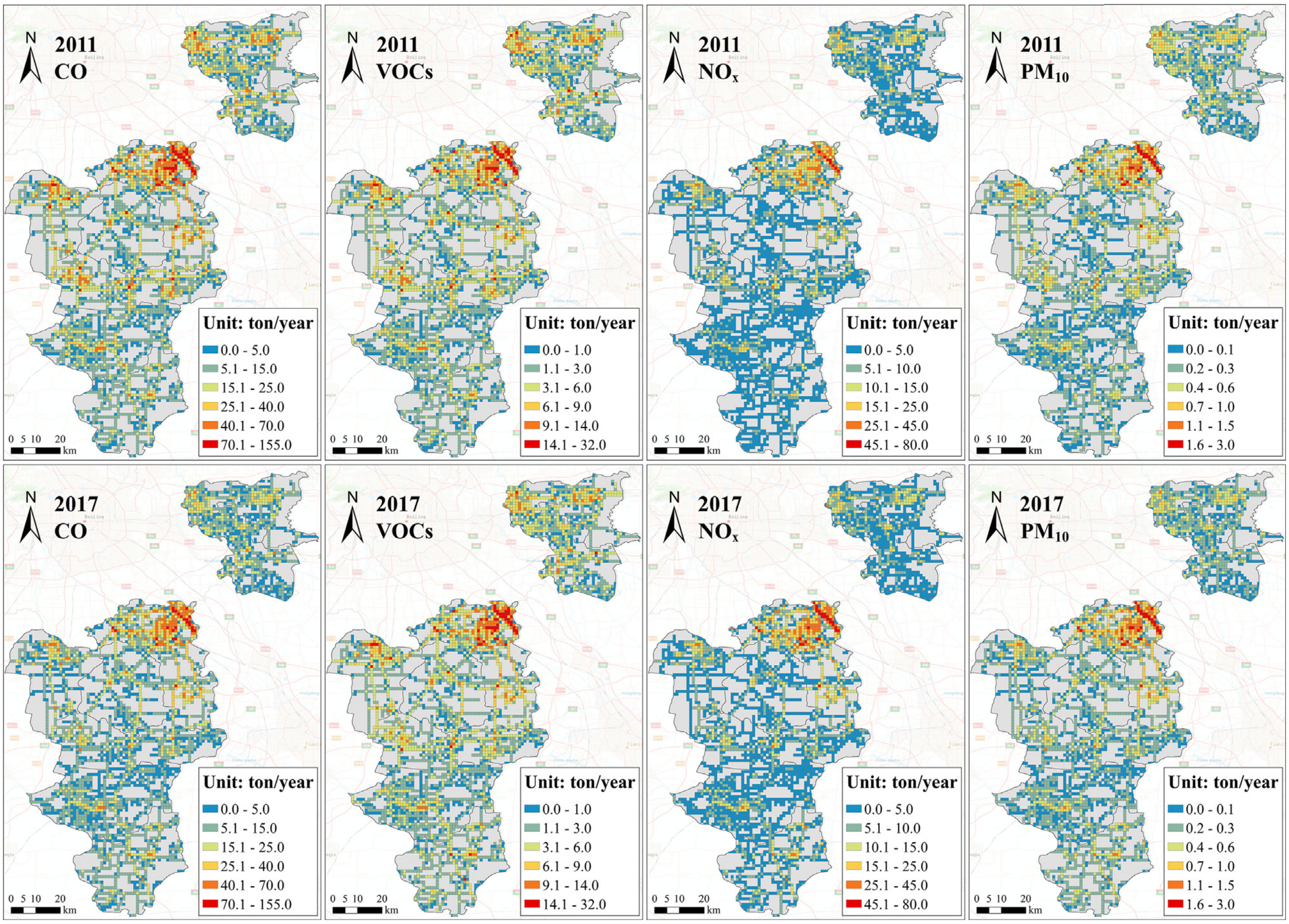

Fig. 9. Spatial distributions of vehicle emissions with 0.01° × 0.01° resolution in Langfang for years 2011 and 2017.

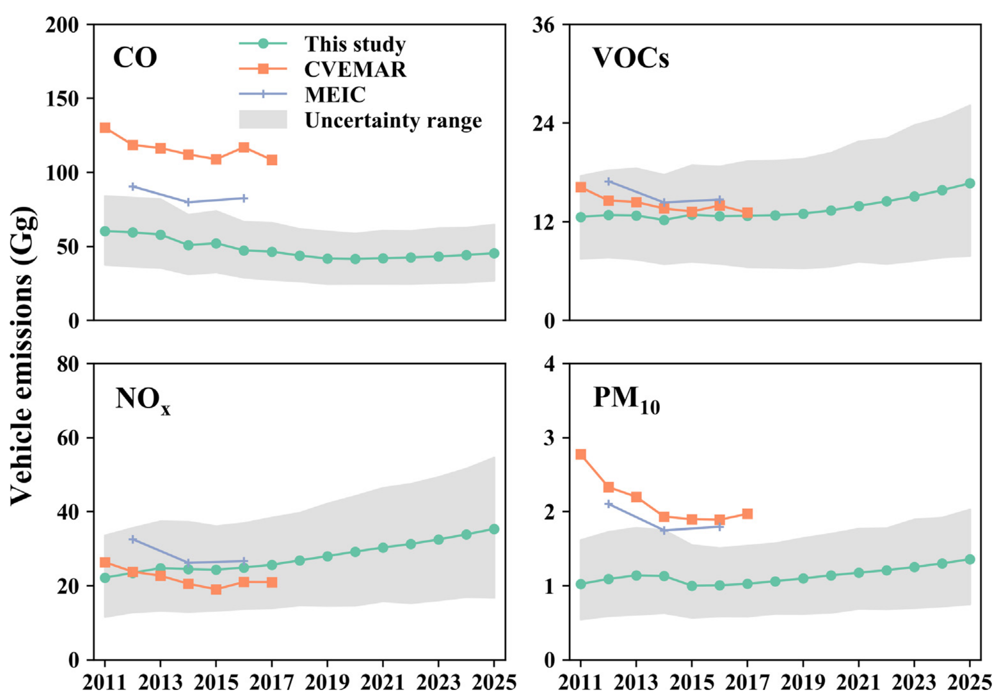

Fig. 10. Vehicle emissions with uncertainty ranges (at a 95% confidence level) in Langfang from 2011 to 2025 and comparison with previous studies.

Table 3
Average uncertainty ranges (at a 95% confidence level) of vehicle emissions in Langfang from 2011 to 2025 (%).

Vehicle type	CO	VOCs	NO_x	PM_{10}
LDV	(−67.9, 72.2)	(−68.1, 72.7)	(−67.8, 72.7)	(−69.9, 84.4)
HDV	(−25.7, 29.5)	(−25.8, 29.6)	(−26.6, 30.9)	(−38.0, 51.3)
LDT	(−68.8, 74.5)	(−68.7, 73.7)	(−69.2, 75.8)	(−71.7, 92.8)
HDT	(−86.9, 91.2)	(−86.9, 92.3)	(−87.2, 92.7)	(−87.7, 107.8)
MC	(−52.8, 60.7)	(−52.6, 60.4)	(−52.8, 60.9)	(−58.7, 81.1)
Total	(−39.7, 41.6)	(−47.5, 50.0)	(−47.7, 50.9)	(−43.7, 51.5)

Environmental Management Annual Report (CVEMAR, released by MEE (2011–2018)) and the Multi-resolution Emission Inventory for China (MEIC, available at http://www.meicmodel.org/, He (2012)).

The VOCs and NO_x emissions in this study are close to those in CVEMAR and MEIC, but the CO and PM_{10} emissions are significantly lower. The emissions of all pollutants are lower in this study than those in MEIC, because the transportation sector in MEIC includes all on-road (covered by this study) and off-road (locomotive, agricultural machinery, construction machinery, etc.) mobile source (Li et al., 2019). The lower estimations of CO and PM_{10} emissions compared to CVEMAR have been reported by Cai and Xie (2013). These differences are caused by a combined effect of different EFs and activity estimations, which will be investigated in future studies.

Table 3 shows the average uncertainty ranges (at a 95% confidence level) during the study period, with the ranges of −39.7%~41.6%, −47.5%~50.0%, −47.7%~50.9%, and −43.7%~51.5% for total CO, VOCs, NO_x, and PM_{10} emissions, respectively. The annual uncertainty ranges are presented in Table S6. From a pollutant perspective, the uncertainties are slightly larger for PM_{10} than other pollutants due to its high CV. For vehicle types, the uncertainties in pollutants emitted by HDT are higher than other vehicle types, because the VKT of HDT (CV of 52.7%) is more uncertain than that of LDV (41.2%), HDV (11.8%), LDT (41.4%), and MC (30.0%). The individual VKT for HDT fluctuates significantly because the HDT is most often used in long-distance transport that is influenced by various factors, such as cargo type (coal, ore, wood, etc.) and service scope (inter-city or inter-province).

There are varying degrees of uncertainties in different input data. The emission uncertainties caused by VKT (CV of 11.8–52.7%) and EF (17–59%) are higher than those by VP (5–10%). Compare with previous studies, the uncertainties in the three parameters are lowered: (1) the VP obtained by VRD provides more detailed information; (2) the VKT determined by survey data reflects more accurate vehicle activity; and (3) the EF simulated by GEI is more consistent with the reality in China. More accurate and detailed data on VKT and EF should be used in further studies.

Although there are some uncertainties, this comprehensive study on vehicle emissions, including data collection, method improvement, trends analysis, policy evaluation, spatial allocation, and uncertainties quantification, would still provide valuable information for environmental policy formulation, especially in middle-sized cities in China.

4. Policy implications

Although a series of control policies have been implemented, vehicle emissions are still high in Langfang. In the future, vehicle emissions may increase more rapidly in Langfang than in Beijing and Tianjin. Based on the results in previous sections, this study proposes the following suggestions to control the emissions effectively in middle-sized cities.

Updating emission standards, scrapping high-emissions vehicles, and improving fuel quality are three major control policies in the past few years (Du et al., 2017; Liu et al., 2017b; Zhang et al., 2014a). The stringent emission standards significantly contribute to the reductions in most pollutants. However, there are two things to note. First, the past emission standards mainly focused on exhaust emissions control, but pay little attention to the evaporative emissions that are also an important VOCs source (Liu et al., 2015). Second, the increasing emission standards have a limited effect on reductions in NO_x emissions (Shen et al., 2015). The China VI standard is expected to solve these problems and should be implemented immediately (Wu et al., 2017). Scrapping high-emissions vehicles before their mandatory scrappage deadlines is an effective policy in the early stage but may be offset over time due to the dwindling high-emissions vehicles (Guo et al., 2016). Higher fuel quality is conducive to the reduction, but the reduction potential would be very limited in the future (Wang et al., 2016). More innovative and comprehensive policies should be formulated and implemented.

The increasing VP is dominated by LDV, for which there are three control policies: constraining VP, promoting public transportation, and popularizing new energy vehicles. Constraining VP is an effective policy to simultaneously reduce emissions, conserve energy and ease congestion, which is demonstrated by megacities. The positive effects are also observed in the middle-sized city (under the VPC), especially for controlling VOCs emissions. Promoting public transportation may help to lower the activity of LDV, and then reduces their emissions. The public transportation is encouraged to develop at national and city levels and has become highly developed in most megacities in China, such as Beijing, Shanghai, and Guangzhou (Peng et al., 2015). However, public transportation is still less developed in middle-sized cities (NBSC, 2012-2018a), indicating great reduction potentials of vehicle emissions (especially for CO and VOCs, under the PTP). The new energy vehicles (refers to the battery electric vehicles and fuel cell vehicles in this study) are zero-emissions vehicles, which is specifically conducive to improve air quality. The government sets targets for promoting the new energy vehicle industry in the next decade (MIIT, 2019). Popularizing new energy vehicles generates long-term gains for emission reductions (especially for VOCs and NO_x, under the NEP), which should receive more attention.

LDT and HDT are major contributors to all pollutants and should be controlled immediately. They are critical to boosting economic prosperity because highway traffic still dominates freight transportation. The emissions of LDT and HDT are bound to increase with the freight volumes in the future (Lang et al., 2016). Optimizing the structures of freight transportation is an effective way to meet this challenge. Especially in Langfang, bordered by two megacities, the share of highway transportation is expected to increase continuously without the optimization (LMBS, 2012-2018). Railway and waterway transportation should be promoted to tackle the rigid demands of freight transportation, especially for long-distance (Song et al., 2018). With these adjustments and optimizations, the significant emission reductions are observed (under the FTO) for most pollutants (CO, NO_x, and PM_{10}), suggesting this policy should be implemented as soon as possible.

To summarize, in addition to conventional control policies, more comprehensive policies should be introduced in middle-sized cities. Constraining VP, promoting public transportation, and popularizing new energy vehicles are three effective policies to tackle the increasing emissions caused by LDV. Optimizing freight transportation structures is the solution to reduce emissions from LDT and HDT. Ideally, the vehicle emissions would be reduced most significantly (under the IS) by adopting all control policies mentioned above, which reveals the maximum reduction potential.

5. Summary and conclusions

A comprehensive study is conducted to investigate the characteristics of vehicle emissions in Langfang, a typical middle-sized city, and provides references to further studies and future policies in middle-sized cities. Also, the SCC method is introduced to improve the original speed correction method in GEI.

In Langfang, except for CO, all vehicle emissions were increased from 2011 to 2017. And in the future, emissions may increase more rapidly than megacities. The conventional policies, such as scrapping high-emissions vehicles, may be offset in the future. Four new possible control policies are evaluated, including VPC, PTP, NEP, and FTO. The most significant emission reductions are observed under the FTO for CO, NO_x, and PM_{10}, and under the VPC for VOCs. Optimizing freight transportation structures could produce co-reduction effects and should be implemented as soon as possible. Constraining VP is an effective way to control the increasing emissions from LDV, which is demonstrated by megacities. The amount and composition of emissions show a significant discrepancy at county level, indicating local conditions should be considered in policy formulation in addition to national consistency. The gridded emissions are distributed consistent with road network, clustered on freeways and arterials, and concentrated in city centers. Multiple surrogates are considered in spatial allocation, which provides more accurate information than single surrogate. Compared with previous studies, more detailed input data is used for lowering emission uncertainties.

Influenced by policy lags, vehicle pollution may become more serious in middle-sized cities than in megacities. Therefore, besides the conventional policies, more innovative and comprehensive control policies should be formulated and implemented. Constraining VP, promoting public transportation, popularizing new energy vehicles, and optimizing freight transportation structures are recognized as promising ways to tackle vehicle pollution in the future. In further studies, cost-effectiveness analysis should be conducted with more accurate and detailed data to identify the optimal combination of these control policies.

CRediT authorship contribution statement

Shida Sun: Writing - original draft, Investigation, Conceptualization, Methodology, Software, Validation, Formal analysis, Writing - review & editing. **Jiaxin Jin:** Investigation, Conceptualization, Formal analysis. **Men Xia:** Writing - original draft, Methodology, Validation. **Yiming Liu:** Writing - original draft, Methodology, Validation. **Meng Gao:** Writing - original draft, Methodology. **Chao Zou:** Software. **Ting Wang:** Data curation. **Yingchao Lin:** Data curation. **Lin Wu:** Data curation. **Hongjun Mao:** Supervision, Project administration, Funding acquisition. **Peng Wang:** Writing - original draft, Investigation, Conceptualization, Methodology, Validation, Writing - review & editing, Supervision.

Declaration of Competing Interest

The authors declare that they have no known competing financial interests or personal relationships that could have appeared to influence the work reported in this paper.

Acknowledgments

This work was funded by the National Natural Science Foundation of China (21607081) and the National key research and development program of China (2017YFC0212104).

Appendix A. Supplementary material

Supplementary data to this article can be found online at https://doi.org/10.1016/j.envint.2020.105514.

References

Alam, M.S., Duffy, P., Hyde, B., McNabola, A., 2018. Downscaling national road transport emission to street level: a case study in Dublin Ireland. J. Clean Prod. 183, 797–809.
Anenberg, S.C., Miller, J., Minjares, R., Du, L., Henze, D.K., Lacey, F., Malley, C.S., Emberson, L., Franco, V., Klimont, Z., Heyes, C., 2017. Impacts and mitigation of excess diesel-related NO_x emissions in 11 major vehicle markets. Nature 545, 467–471.
BMSTC, 2018. The management measure for promoting new energy vehicles in Beijing. Beijing Municipal Sci. Technol. Commission.
Cai, H., Xie, S., 2007. Estimation of vehicular emission inventories in China from 1980 to 2005. Atmos. Environ. 41, 8963–8979.
Cai, H., Xie, S., 2013. Temporal and spatial variation in recent vehicular emission inventories in China based on dynamic emission factors. J. Air Waste Manag. Assoc. 63, 310–326.
CATARC. China Automotive Industry Yearbooks. http://data.cnki.net/Yearbook/Navi?type=type&code=A: China Automotive Technology and Research Center Co.,Ltd.; 2012–2018.
Chang, X., Wang, S., Zhao, B., Cai, S., Hao, J., 2018. Assessment of inter-city transport of particulate matter in the Beijing-Tianjin-Hebei region. Atmos. Chem. Phys. 18, 4843–4858.
Du, H., Liu, D., Southworth, F., Ma, S., Qiu, F., 2017. Pathways for energy conservation and emissions mitigation in road transport up to 2030: a case study of the Jing-Jin-Ji area China. J. Clean Prod. 162, 882–893.
Fang, X., Bi, X., Xu, H., Wu, J., Zhang, Y., Feng, Y., 2017. Source apportionment of ambient PM_{10} and $PM_{2.5}$ in Haikou. China. Atmos. Res. 190, 1–9.
Gong, M., Yin, S., Gu, X., Xu, Y., Jiang, N., Zhang, R., 2017. Refined 2013-based vehicle emission inventory and its spatial and temporal characteristics in Zhengzhou. China. Sci. Total Environ. 599–600, 1149–1159.
GOSC. The three-year action plan for optimizing freight transportation structure (2018-2020). http://www.gov.cn/zhengce/content/2018-10/09/content_5328817.htm: General Office of the State Council; 2018.
Guo, X., Fu, L., Ji, M., Lang, J., Chen, D., Cheng, S., 2016. Scenario analysis to vehicular emission reduction in Beijing-Tianjin-Hebei (BTH) region China. Environ. Pollut. 216, 470–479.
Hao, Y., Song, X., 2018. Research on trends and spatial distribution of vehicular emissions and its control measure assessment in the Yangtze River Delta, China, for 1999–2015. Environ. Sci. Pollut. Res. 25, 36503–36517.
He, J., Wu, L., Mao, H., Liu, H., Jing, B., Yu, Y., Ren, P., Feng, C., Liu, X., 2016. Development of a vehicle emission inventory with high temporal-spatial resolution based on NRT traffic data and its impact on air pollution in Beijing – Part 2: Impact of vehicle emission on urban air quality. Atmos. Chem. Phys. 16, 3171–3184.
He, K., 2012. Multi-resolution Emission Inventory for China (MEIC): model framework and 1990–2010 anthropogenic emissions. AGU Fall Meet.
He, K., Huo, H., Zhang, Q., He, D., An, F., Wang, M., Walsh, M.P., 2005. Oil consumption and CO_2 emissions in China's road transport: current status, future trends, and policy implications. Energy Policy 33, 1499–1507.
HPBS. Hebei Economic Yearbook. http://www.hetj.gov.cn/hetj/tjsj/jjnj/: Hebei Provincial Bureau of Statistics; 2012-2018.
Huang, C., Tao, S., Lou, S., Hu, Q., Wang, H., Wang, Q., Li, L., Wang, H., Quan, Y., Zhou, L., 2017. Evaluation of emission factors for light-duty gasoline vehicles based on chassis dynamometer and tunnel studies in Shanghai China. Atmos. Environ. 169, 193–203.
Huang, C., Wang, H.L., Li, L., Wang, Q., Lu, Q., de Gouw, J.A., Zhou, M., Jing, S.A., Lu, J., Chen, C.H., 2015. VOC species and emission inventory from vehicles and their SOA formation potentials estimation in Shanghai. China. Atmos. Chem. Phys. 15, 11081–11096.
Huo, H., Zhang, Q., He, K., Yao, Z., Wang, M., 2012. Vehicle-use intensity in China: current status and future trend. Energy Policy 43, 6–16.
Huo, H., Zhang, Q., He, K., Yao, Z., Wang, X., Zheng, B., Streets, D.G., Wang, Q., Ding, Y., 2011. Modeling vehicle emissions in different types of Chinese cities: importance of vehicle fleet and local features. Environ. Pollut. 159, 2954–2960.
IPCC. 2006 IPCC Guidelines for National Greenhouse Gas Inventories – Chapter 3: Uncertainties. https://www.ipcc-nggip.iges.or.jp/public/2006gl/pdf/1_Volume1/V1_3_Ch3_Uncertainties.pdf: Intergovernmental Panel on Climate Change; 2006.
Jia, T., Li, Q., Shi, W., 2018. Estimation and analysis of emissions from on-road vehicles in Mainland China for the period 2011–2015. Atmos. Environ. 191, 500–512.
Jing, B., Wu, L., Mao, H., Gong, S., He, J., Zou, C., Song, G., Li, X., Wu, Z., 2016. Development of a vehicle emission inventory with high temporal-spatial resolution based on NRT traffic data and its impact on air pollution in Beijing – Part 1: Development and evaluation of vehicle emission inventory. Atmos. Chem. Phys. 16, 3161–3170.
Lang, J., Cheng, S., Wei, W., Zhou, Y., Wei, X., Chen, D., 2012. A study on the trends of vehicular emissions in the Beijing-Tianjin-Hebei (BTH) region China. Atmos. Environ. 62, 605–614.
Lang, J., Cheng, S., Zhou, Y., Zhang, Y., Wang, G., 2014. Air pollutant emissions from on-road vehicles in China, 1999–2011. Sci. Total Environ. 496, 1–10.
Lang, J., Zhou, Y., Cheng, S., Zhang, Y., Dong, M., Li, S., Wang, G., Zhang, Y., 2016. Unregulated pollutant emissions from on-road vehicles in China, 1999–2014. Sci. Total Environ. 573, 974–984.
Li, L., Ge, Y., Wang, M., Li, J., Peng, Z., Song, Y., Zhang, L., 2015. Effect of gasoline/methanol blends on motorcycle emissions: exhaust and evaporative emissions. Atmos. Environ. 102, 79–85.
Li, M., Zhang, Q., Zheng, B., Tong, D., Lei, Y., Liu, F., Hong, C., Kang, S., Yan, L., Zhang, Y., Bo, Y., Su, H., Cheng, Y., He, K., 2019. Persistent growth of anthropogenic non-methane volatile organic compound (NMVOC) emissions in China during 1990–2017: drivers, speciation and ozone formation potential. Atmos. Chem. Phys. 19, 8897–8913.
Li, R., Wu, L., Mao, H., He, J., Jing, B., Zou, C., 2016. Establishment of an air pollutant emission inventory for Langfang urban area. Acta Sci. Circumst. 36, 3527–3534.
Li, S., Lang, J., Zhou, Y., Liang, X., Chen, D., Wei, P., 2020. Trends in ammonia emissions from light-duty gasoline vehicles in China, 1999–2017. Sci. Total Environ. 700, 134359.
Liu, H., Man, H., Tschantz, M., Wu, Y., He, K., Hao, J., 2015. VOC from vehicular

evaporation emissions: status and control strategy. Environ. Sci. Technol. 49, 14424–14431.
Liu, Y.H., Liao, W.Y., Li, L., Huang, Y.T., Xu, W.J., 2017a. Vehicle emission trends in China's Guangdong Province from 1994 to 2014. Sci. Total Environ. 586, 512–521.
Liu, Y.H., Liao, W.Y., Lin, X.F., Li, L., Zeng, X.L., 2017b. Assessment of Co-benefits of vehicle emission reduction measures for 2015–2020 in the Pearl River Delta region China. Environ. Pollut. 223, 62–72.
Liu, Y.H., Ma, J.L., Li, L., Lin, X.F., Xu, W.J., Ding, H., 2018. A high temporal-spatial vehicle emission inventory based on detailed hourly traffic data in a medium-sized city of China. Environ. Pollut. 236, 324–333.
LMBS. Economic Statistical Yearbook of Langfang. http://www.lf.gov.cn/Category_365/Index.aspx: Langfang Municipal Bureau of Statistics; 2012-2018.
Lv, W., Hu, Y., Li, E., Liu, H., Pan, H., Ji, S., Hayat, T., Alsaedi, A., Ahmad, B., 2019. Evaluation of vehicle emission in Yunnan province from 2003 to 2015. J. Clean Prod. 207, 814–825.
MEE. China Vehicle Environmental Management Annual Report. http://www.vecc-mep.org.cn/huanbao/: Ministry of Ecology and Environment; 2011-2018.
MEE. The Announcement about Releasing Five National Technical Guidelines of the Air Pollutant Emissions Inventory. http://www.mee.gov.cn/gkml/hbb/bgg/201501/t20150107_293955.htm: Ministry of Ecology Environment; 2014.
MIIT. The development plan for the new energy vehicle industry (2021-2035). http://www.miit.gov.cn/n1278117/n1648113/c7553623/content.html: Ministry of Industry and Information Technology; 2019.
Mohammadiha, A., Malakooti, H., Esfahanian, V., 2018. Development of reduction scenarios for criteria air pollutants emission in Tehran Traffic Sector. Iran. Sci. Total Environ. 622–623, 17–28.
NBSC. China City Statistical Yearbook. http://www.stats.gov.cn/tjsj/tjcbw/201907/t20190708_1674721.html: National Bureau of Statistics of China; 2012-2018a.
NBSC. China Statistical Yearbook. http://www.stats.gov.cn/tjsj/ndsj/: National Bureau of Statistics of China; 2012-2018b.
Peng, B., Du, H., Ma, S., Fan, Y., Broadstock, D.C., 2015. Urban passenger transport energy saving and emission reduction potential: a case study for Tianjin China. Energy Conv. Manag. 102, 4–16.
PGHP. The 13th Five-Year Plan for developing integrated transport system in Hebei Province. http://www.hebei.gov.cn/hebei/10731222/10751796/10758975/13999016/index.html: The People's Government of Hebei Province. 2017.
Pu, Y., Yang, C., Liu, H., Chen, Z., Chen, A., 2015. Impact of license plate restriction policy on emission reduction in Hangzhou using a bottom-up approach. Transport. Res. Part D-Transport. Environ. 34, 281–292.
Shen, X., Yao, Z., Zhang, Q., Wagner, D.V., Huo, H., Zhang, Y., Zheng, B., He, K., 2015. Development of database of real-world diesel vehicle emission factors for China. J. Environ. Sci. 31, 209–220.
Song, C., Liu, B., Dai, Q., Li, H., Mao, H., 2019. Temperature dependence and source apportionment of volatile organic compounds (VOCs) at an urban site on the north China plain. Atmos. Environ. 207, 167–181.
Song, C., Ma, C., Zhang, Y., Wang, T., Wu, L., Wang, P., Liu, Y., Li, Q., Zhang, J., Dai, Q., Zou, C., Sun, L., Mao, H., 2018. Heavy-duty diesel vehicles dominate vehicle emissions in a tunnel study in northern China. Sci. Total Environ. 637–638, 431–442.
Song, X., Hao, Y., Zhang, C., Peng, J., Zhu, X., 2016. Vehicular emission trends in the Pan-Yangtze River Delta in China between 1999 and 2013. J. Clean Prod. 137, 1045–1054.
Streets, D.G., Fu, J.S., Jang, C.J., Hao, J., He, K., Tang, X., Zhang, Y., Wang, Z., Li, Z., Zhang, Q., Wang, L., Wang, B., Yu, C., 2007. Air quality during the 2008 Beijing Olympic Games. Atmos. Environ. 41, 480–492.
Suarez-Bertoa, R., Mendoza-Villafuerte, P., Bonnel, P., Lilova, V., Hill, L., Perujo, A., Astorga, C., 2016. On-road measurement of NH_3 and N_2O emissions from a Euro V heavy-duty vehicle. Atmos. Environ. 139, 167–175.
Sun, S., Zhao, G., Wang, T., Jin, J., Wang, P., Lin, Y., Li, H., Ying, Q., Mao, H., 2019. Past and future trends of vehicle emissions in Tianjin, China, from 2000 to 2030. Atmos. Environ. 209, 182–191.
Sun, S.D., Jiang, W., Gao, W.D., 2016. Vehicle emission trends and spatial distribution in Shandong province, China, from 2000 to 2014. Atmos. Environ. 147, 190–199.
Sun, S.D., Jiang, W., Gao, W.D., 2017. Vehicle emission inventory and spatial distribution in Qingdao. CHINA Environ. Sci. 37, 49–59.
Vouitsis, E., Ntziachristos, L., Pistikopoulos, P., Samaras, Z., Chrysikou, L., Samara, C., Papadimitriou, C., Samaras, P., Sakellaropoulos, G., 2009. An investigation on the physical, chemical and ecotoxicological characteristics of particulate matter emitted from light-duty vehicles. Environ. Pollut. 157, 2320–2327.
Wang, H., Chen, C., Huang, C., Fu, L., 2008. On-road vehicle emission inventory and its uncertainty analysis for Shanghai. China. Sci. Total Environ. 398, 60–67.
Wang, H., Fu, L., Bi, J., 2011. CO_2 and pollutant emissions from passenger cars in China. Energy Policy 39, 3005–3011.
Wang, H., Fu, L., Zhou, Y., Du, X., Ge, W., 2010. Trends in vehicular emissions in China's mega cities from 1995 to 2005. Environ. Pollut. 158, 394–400.
Wang, Y., Zheng, R., Qin, Y., Peng, J., Li, M., Lei, J., Wu, Y., Hu, M., Shuai, S., 2016. The impact of fuel compositions on the particulate emissions of direct injection gasoline engine. Fuel 166, 543–552.
Wu, X., Wu, Y., Zhang, S., Liu, H., Fu, L., Hao, J., 2016. Assessment of vehicle emission programs in China during 1998–2013: achievement, challenges and implications. Environ. Pollut. 214, 556–567.
Wu, X., Zhang, S., Wu, Y., Li, Z., Zhou, Y., Fu, L., Hao, J., 2015. Real-world emissions and fuel consumption of diesel buses and trucks in Macao: From on-road measurement to policy implications. Atmos. Environ. 120, 393–403.
Wu, Y., Zhang, S., Hao, J., Liu, H., Wu, X., Hu, J., Walsh, M.P., Wallington, T.J., Zhang, K.M., Stevanovic, S., 2017. On-road vehicle emissions and their control in China: a review and outlook. Sci. Total Environ. 574, 332–349.
Wu, Y., Zhang, S.J., Li, M.L., Ge, Y.S., Shu, J.W., Zhou, Y., Xu, Y.Y., Hu, J.N., Liu, H., Fu, L.X., He, K.B., Hao, J.M., 2012. The challenge to NO_x emission control for heavy-duty diesel vehicles in China. Atmos. Chem. Phys. 12, 9365–9379.
Xu, W., Sun, J., Liu, Y., Xiao, Y., Tian, Y., Zhao, B., Zhang, X., 2019. Spatiotemporal variation and socioeconomic drivers of air pollution in China during 2005–2016. J. Environ. Manage. 245, 66–75.
Yang, W., Zhang, Q., Wang, J., Zhou, C., Zhang, Y., Pan, Z., 2018. Emission characteristics and ozone formation potentials of VOCs from gasoline passenger cars at different driving modes. Atmos. Pollut. Res. 9, 804–813.
Zhang, Q.Y., Li, X.X., Tian, W.L., Fu, A.Y., Du, W.F., Wang, C., 2014a. Scenarios for vehicular air pollutant emissions abatement: a case study in Hangzhou, China. J. Zhejiang Univ. Sci. A 15 (9), 753–760.
Zhang, S., Wu, Y., Liu, H., Wu, X., Zhou, Y., Yao, Z., Fu, L., He, K., Hao, J., 2013. Historical evaluation of vehicle emission control in Guangzhou based on a multi-year emission inventory. Atmos. Environ. 76, 32–42.
Zhang, S., Wu, Y., Wu, X., Li, M., Ge, Y., Liang, B., Xu, Y., Zhou, Y., Liu, H., Fu, L., Hao, J., 2014b. Historic and future trends of vehicle emissions in Beijing, 1998–2020: a policy assessment for the most stringent vehicle emission control program in China. Atmos. Environ. 89, 216–229.
Zhao, B., Wang, P., Ma, J.Z., Zhu, S., Pozzer, A., Li, W., 2012. A high-resolution emission inventory of primary pollutants for the Huabei region. China. Atmos. Chem. Phys. 12, 481–501.
Zhao, J., Zhang, J., Sun, L., Liu, Y., Lin, Y., Li, Y., Wang, T., Mao, H., 2018. Characterization of $PM_{2.5}$-bound nitrated and oxygenated polycyclic aromatic hydrocarbons in ambient air of Langfang during periods with and without traffic restriction. Atmos. Res. 213, 302–308.
Zheng, B., Zhang, Q., Borken-Kleefeld, J., Huo, H., Guan, D., Klimont, Z., Peters, G.P., He, K., 2015. How will greenhouse gas emissions from motor vehicles be constrained in China around 2030? Appl. Energy 156, 230–240.
Zheng, J., Che, W., Wang, X., Louie, P., Zhong, L., 2012. Road-network-based spatial allocation of on-road mobile source emissions in the pearl river delta region, China, and comparisons with population-based approach. J. Air Waste Manag. Assoc. 59, 1405–1416.